AMERICAN SOCIETY FOR MICROBIOLOGY | Infection and Immunity®

BACTERIAL INFECTIONS

The AmiC/NlpD Pathway Dominates Peptidoglycan Breakdown in *Neisseria meningitidis* and Affects Cell Separation, NOD1 Agonist Production, and Infection

Jia Mun Chan,[a] Kathleen T. Hackett,[a] Katelynn L. Woodhams,[a] Ryan E. Schaub,[a] Joseph P. Dillard[a]

[a]University of Wisconsin—Madison, Department of Medical Microbiology and Immunology, School of Medicine and Public Health, Madison, Wisconsin, USA

ABSTRACT The human-restricted pathogen *Neisseria meningitidis*, which is best known for causing invasive meningococcal disease, has a nonpathogenic lifestyle as an asymptomatic colonizer of the human naso- and oropharyngeal space. *N. meningitidis* releases small peptidoglycan (PG) fragments during growth. It was demonstrated previously that *N. meningitidis* releases low levels of tripeptide PG monomer, which is an inflammatory molecule recognized by the human intracellular innate immune receptor NOD1. In the present study, we demonstrated that *N. meningitidis* released more PG-derived peptides than PG monomers. Using a reporter cell line overexpressing human NOD1, we showed that *N. meningitidis* activates NOD1 using PG-derived peptides. The generation of such peptides required the presence of the periplasmic *N*-acetylmuramyl-L-alanine amidase AmiC and the outer membrane lipoprotein NlpD. AmiC and NlpD were found to function in cell separation, and mutation of either *amiC* or *nlpD* resulted in large clumps of unseparated *N. meningitidis* cells instead of the characteristic diplococci. Using stochastic optical reconstruction microscopy, we demonstrated that FLAG epitope-tagged NlpD localized to the septum, while similarly tagged AmiC was found at the septum in some diplococci but was distributed around the cell in most cases. In a human whole-blood infection assay, an *nlpD* mutant was severely attenuated and showed particular sensitivity to complement. Thus, in *N. meningitidis*, the cell separation proteins AmiC and NlpD are necessary for NOD1 stimulation and survival during infection of human blood.

KEYWORDS *Neisseria meningitidis*, peptidoglycan hydrolysis, AmiC, NlpD, NOD1, amidase, peptidoglycan, peptidoglycan hydrolases

Neisseria meningitidis, also known as the meningococcus, is an obligate colonizer of the human nasopharyngeal space. Meningococci occasionally disseminate to cause invasive disease such as meningitis and septicemia. Invasive disease has a fatality rate of around 11% even with early treatment, and 11 to 19% of survivors develop lifelong sequelae (1–3). *N. meningitidis* colonizes up to 25% of the population at any one time (3). The carriage rate of *N. meningitidis* can be as high as 70% in areas of high density such as military barracks and college dormitories and during the Hajj pilgrimage (3, 4); prolonged exposure to carriers increases the risk of invasive meningococcal disease for noncarriers (4). *N. meningitidis* encodes multiple virulence factors that allow it to invade the bloodstream and cross the blood-brain barrier, cause a large inflammatory response, and evade clearance by the immune system (5, 6). Much of the tissue damage sustained during meningococcal disease is a result of a strong inflammatory immune response (3, 6, 7). One class of immunostimulatory molecules made and released by *N. meningitidis* is diaminopimelic acid (DAP)-type peptidoglycan (PG) fragments (8).

PG is a structural macromolecule that confers bacterial cell shape and protects the cell against turgor pressure. It is made of repeating subunits of *N*-acetylglucosamine (GlcNAc) and *N*-acetylmuramic acid (MurNAc), with peptide chains attached to the *N*-acetylmuramic

Editor Igor E. Brodsky, University of Pennsylvania

Address correspondence to Joseph P. Dillard, joe.dillard@wisc.edu.

The authors declare no conflict of interest.

Received 1 September 2021
Returned for modification 9 October 2021
Accepted 18 January 2022

Accepted manuscript posted online 14 February 2022
Published 17 March 2022

acid moiety (9). The third amino acid on this peptide chain is DAP in most Gram-negative bacteria and Gram-positive bacilli and lysine in most other Gram-positive bacteria (10). The breakdown of existing PG strands and the incorporation of newly synthesized PG strands allow cell enlargement and cell separation (11), and this process generates small PG fragments as the bacteria grow (12, 13). Most Gram-negative bacteria release very small amounts of PG fragments; instead, PG fragments are typically contained in the periplasmic space and efficiently taken back into the cytoplasm by a PG fragment permease in order to be reused in cellular processes (13, 14). A limited group of Gram-negative bacteria, including but not limited to *N. meningitidis*; the closely related pathogen *Neisseria gonorrhoeae*; the etiological agent of whooping cough, *Bordetella pertussis*; and the squid symbiont *Vibrio fischeri*, release cytotoxic PG monomers (GlcNAc-anhydroMurNAc-peptide) with no overt effects on bacterial growth (8, 12, 15, 16). PG monomers released from *N. gonorrhoeae* cause ciliated cell death in human Fallopian tubes (15, 17). In addition to releasing PG monomers, *N. meningitidis* also releases PG dimers (two glycosidically linked or peptide-linked monomers) and PG-derived sugars such as GlcNAc-anhydroMurNAc disaccharide and anhydroMurNAc (8). The release of PG-derived peptides by *N. meningitidis* has not been characterized.

Host organisms such as humans have evolved strategies to detect and respond to microbe-associated molecular patterns to either prevent or resolve an infection. One such intracellular innate immune receptor is human NOD1 (hNOD1). hNOD1 induces a proinflammatory response upon the recognition of PG fragments with a terminal DAP, which includes tripeptide PG monomers (GlcNAc-anhydroMurNAc-L-Ala-D-Glu-*meso*DAP) and PG-derived tripeptide (L-Ala-D-Glu-*meso*DAP) (18–21). hNOD1 does not respond well to amidated PG fragments; some species of Gram-positive bacteria that have DAP-type PG, such as *Bacillus subtilis*, amidate the DAP moiety of their PG stems (19, 20, 22). Thus, hNOD1 predominantly detects the presence of Gram-negative bacteria, including *N. meningitidis*. In this study, we characterized PG-derived peptides released by *N. meningitidis* and found that meningococci release immunologically relevant amounts of hNOD1 activating PG-derived peptides.

RESULTS

The Ltg and AmiC pathways of sacculus degradation. Previous studies of PG fragment breakdown and release by *N. meningitidis*, *N. gonorrhoeae*, and commensal species indicate that PG can be broken down in two different ways (Fig. 1) (15). In the lytic transglycosylase-dominated pathway, LtgA removes peptide-cross-linked dimers from the sacculus, and an endolytic lytic transglycosylase, likely LtgE, creates glycosidically linked dimers (23, 24). After DacB (penicillin binding protein 3 [PBP3]) cuts cross-links between strands, LtgA and LtgD degrade strands to PG monomers (8, 25). LdcA acts on the tetrapeptide PG monomers to convert them to tripeptide PG monomers, thus making them NOD1 agonists (26, 27). For the AmiC-dependent pathway, strand separation by DacB is followed by stripping of the peptides from the strands by AmiC, with NlpD activation (28, 29). AmiC cannot remove the final peptide (28, 30). LtgC then degrades the nearly naked glycan strand, creating free disaccharides and tetrasaccharide-peptide (31, 32). NagZ breaks down the disaccharides into monosaccharides (33), and NlpC is predicted to break down tetrapeptides (34). Although both pathways are active in all *Neisseria* species studied, the lytic transglycosylase pathway is slightly favored in *N. gonorrhoeae*. PG monomers are the most abundant PG fragments released by gonococci, but free tri- and tetrapeptides are almost as abundant as PG monomers (28, 35). In *N. meningitidis*, experiments monitoring [^{3}H]glucosamine-labeled PG suggest that the AmiC pathway is favored. Free sugars and tetrasaccharide-peptide make up a larger proportion of the PG fragments released by *N. meningitidis* than do PG monomers and dimers (8). If *N. meningitidis* extensively uses the AmiC pathway, then this species may make significant amounts of a NOD1 agonist in the form of free tripeptides.

We examined PG fragment release in *N. meningitidis* using pulse-chase metabolic labeling with [2,6-^{3}H]DAP. PG fragments released into the medium during growth

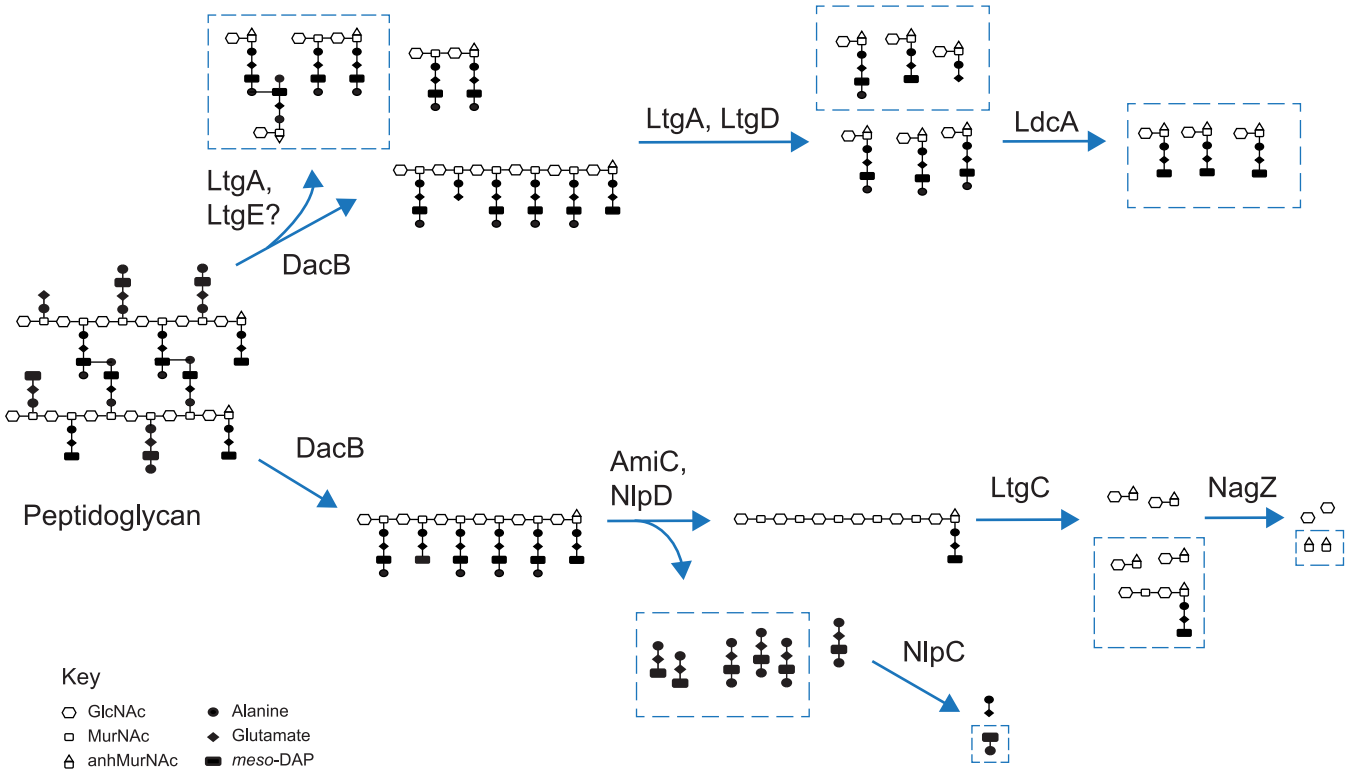

FIG 1 Peptidoglycan degradation pathways in *Neisseria* species. During growth, portions of the sacculus are degraded to allow cell wall enlargement or remodeling. (Top) In the lytic transglycosylase-dominated pathway, PG dimers are liberated by LtgA and LtgE, strands are degraded to monomers by LtgA and LtgD, and a majority of PG monomers have their peptides shortened to 3 amino acids by LdcA. (Bottom) In the amidase-dominated pathway, peptides are removed from PG strands by AmiC, which is activated by NlpD. Free peptides may be further degraded to dipeptides by one of the three NlpC enzymes. LtgC degrades the denuded strand to free disaccharides and tetrasaccharide-peptide. NagZ, a cytosolic enzyme, cleaves the disaccharides into monosaccharides. Molecules shown with boxes around them are released from the bacteria into the milieu.

were analyzed by size exclusion chromatography (Fig. 2A). Five major peaks were observed, and these contain PG dimers, tetrasaccharide-peptide, PG monomers, free tri- and tetrapeptides, and free dipeptides (8, 35). The amounts of PG in the free tri- and tetrapeptide and dipeptide fractions were much larger than those in the PG dimer and monomer fractions. These data indicate that *N. meningitidis* extensively degrades its PG to free peptides and sugars prior to release and that it favors the AmiC-dependent pathway for PG breakdown.

Released tri- and tetrapeptides from PG have been characterized in *N. gonorrhoeae*. Sinha and Rosenthal demonstrated that the peptides were composed of Ala-Glu-DAP and Ala-Glu-DAP-Ala and that they were not cross-linked (35). Lenz et al. found that an *N. gonorrhoeae* mutant defective for *amiC* did not release free tri- and tetrapeptides (28). The second PG-derived peptide peak (dipeptides) has been noted previously but not thoroughly investigated, partly because it overlaps somewhat the peak for free single amino acids not incorporated in the labeling process (Fig. 2A) (12, 36). *Escherichia coli* is known to release the disaccharide DAP-Ala (37). Therefore, we tested whether metabolic labeling with [^{3}H]D-Ala would label the released dipeptide. The incorporation of [^{3}H]D-Ala in this peak was similar to the incorporation of [^{3}H]DAP, indicating that for *N. meningitidis*, as for *E. coli*, the released dipeptide fraction may contain DAP-D-Ala.

Mutation of *amiC* or *nlpD* abolishes peptide release. *N. meningitidis* encodes one periplasmic *N*-acetylmuramyl-L-alanine amidase, AmiC (38). Meningococcal AmiC is predicted to be a 417-amino-acid zinc-dependent metalloprotease with a Tat signal sequence, an N-terminal Amidase N-terminal (AMIN) domain that binds PG, and a C-terminal catalytic domain that cleaves peptide stems. AmiC homologues in *E. coli* and *N. gonorrhoeae* function as cell separation amidases (30, 39). To examine the role of meningococcal AmiC in PG fragment production and release, we generated an

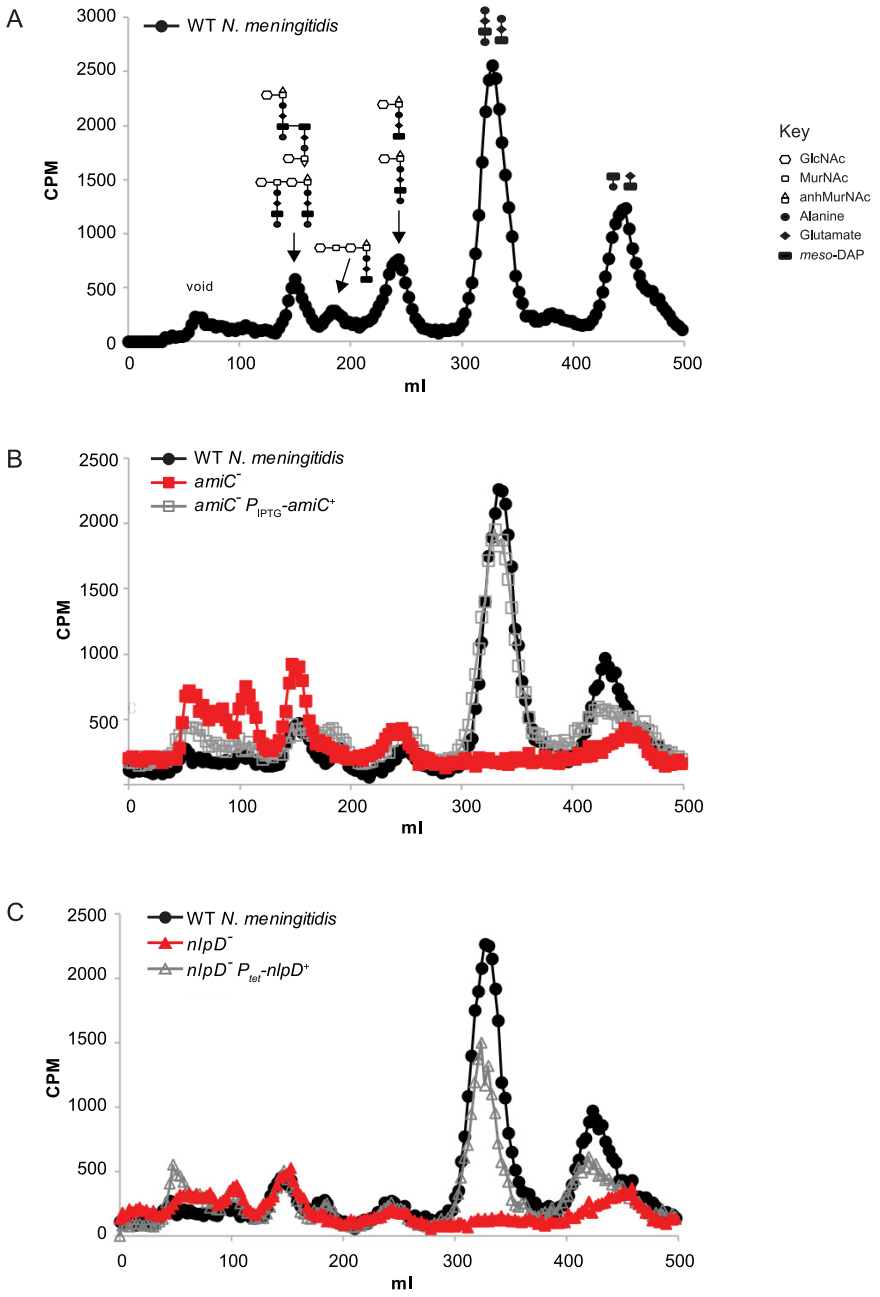

FIG 2 Peptidoglycan fragment release from growing *N. meningitidis* cells. (A) [2,6-^{3}H]DAP-labeled PG fragments released by WT *N. meningitidis* (ATCC 13102 *cap*) were separated by size exclusion chromatography, resolving into five distinct peaks in the included volume. Cartoons above each peak show the structures of the PG fragments, representing, in order from the left, dimers, tetrasaccharide-peptide, monomers, free tetra- and tripeptides, and free dipeptides. The structures of the dipeptides are not yet chemically confirmed. (B) PG fragment release from an *amiC* mutant (KL1065) and its complemented strain (EC1020). (C) PG fragment release from an *nlpD* mutant (KL1072) and its complemented strain (EC1026). Mutation of *amiC* (B) or *nlpD* (C) abolished the release of PG-derived peptides. Genetic complementation of the *amiC* (B) and *nlpD* (C) mutations partially restored the release of PG-derived peptides. The results depicted are representative of data from three experiments.

in-frame markerless deletion of *amiC*. Mutation of *amiC* abolished PG peptide release and resulted in increased PG multimer release (Fig. 2B). If AmiC were able to cleave PG monomers, we would expect to see a proportional increase in PG monomer release with the decrease in peptide release by the *amiC* mutant. However, there is no significant difference in PG monomer release between the wild type (WT) and the *amiC*

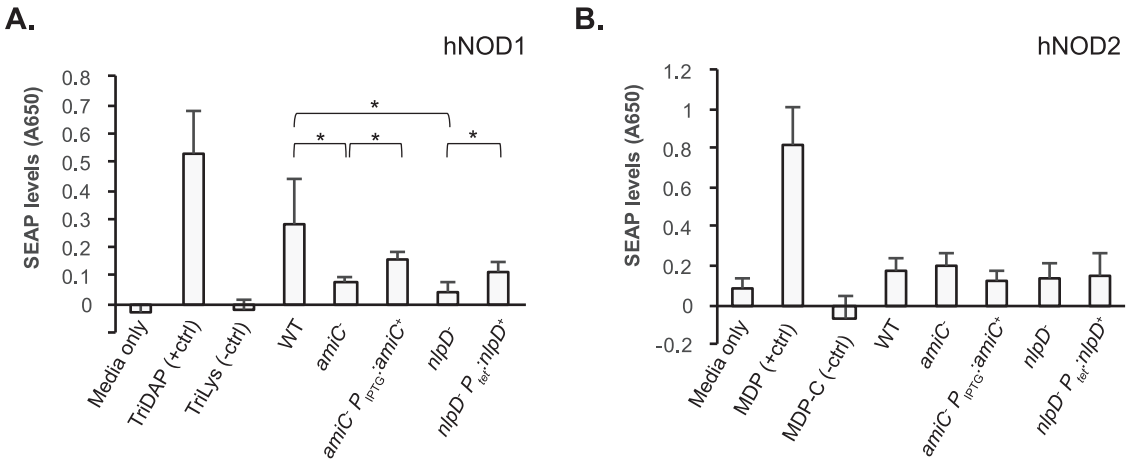

FIG 3 Stimulation of human NOD1 or human NOD2 by conditioned media from *N. meningitidis* mutants that do not release PG-derived peptides. Supernatants from WT (ATCC 13102 *cap*), *amiC* mutant (KL1065), *amiC* complementation (EC1020), *nlpD* mutant (KL1072), and *nlpD* complementation (EC1026) strains were harvested, normalized to total cellular protein, and used to treat HEK293 reporter cell lines overexpressing hNOD1 (A) or hNOD2 (B) as well as parental HEK293 cell lines. hNOD activation was determined by measuring the amount of secreted alkaline phosphatase (SEAP) in the media. The values presented are the SEAP levels measured as the A_{650} for the hNOD-overexpressing strain minus those of the parental strain lacking hNOD overexpression, i.e., A_{650} (hNOD1) $-$ A_{650} (NULL1) or A_{650} (hNOD2) $-$ A_{650} (NULL2). Error bars represent the standard deviations. Results are from four independent experiments, with technical triplicates for each biological replicate. Statistical significance was determined by Student's *t* test, in which * indicates a *P* value of <0.05.

mutant. Complementation of *amiC* from an ectopic locus restored almost WT distributions of released PG fragments. Our results suggest that meningococcal AmiC liberates peptide stems from the sacculi, and it is necessary for the release of both free tri- and tetrapeptides and free dipeptide.

NlpD is a putative AmiC activator protein and functions to potentiate the amidase activity of AmiC in *N. gonorrhoeae* and *E. coli* (28, 29). Meningococcal NlpD is predicted to be a 415-amino-acid outer membrane lipoprotein with two LysM PG binding domains and a degenerate LytM/M23 peptidase domain. Like NlpD homologues from *N. gonorrhoeae* and *E. coli*, only 2/4 of the active-site residues in the M23 peptidase domain of meningococcal NlpD are conserved (29, 40). Analyses of *N. gonorrhoeae* and *E. coli* indicate that their NlpD homologues do not have enzymatic function but instead act as activator proteins for the amidases (28, 29, 40). Mutation of *nlpD* in *N. meningitidis* abolished free peptide release without affecting the release of PG monomers and dimers (Fig. 2C). Complementation of *nlpD* at an ectopic site partially rescued peptide release. We conclude that AmiC and NlpD are indispensable for PG-derived peptide release in *N. meningitidis* and that AmiC activity is dependent on activation by NlpD.

PG-derived peptides released by *N. meningitidis* stimulate NOD1 activation. HEK293 reporter cell lines overexpressing NOD receptors were used to determine if peptide release by meningococci is necessary for the induction of a NOD-dependent response. In this assay, NOD activation is measured by determining the amount of NF-κB-controlled secreted alkaline phosphatase (SEAP) detected in the medium via a colorimetric assay. HEK293 cells overexpressing human NOD1 were treated with the cell-free supernatant from the WT, the *amiC* mutant, the *nlpD* mutant, or induced cultures of the respective *amiC* or *nlpD* complementation strains (Fig. 3A). As described previously and demonstrated here, the supernatant from *N. meningitidis* engenders a NOD1-dependent response (Fig. 3) (8). We found that the supernatant from WT *N. meningitidis* induced 3.6- or 7.5-times-higher levels of human NOD1 activation than an *amiC* or an *nlpD* mutant, respectively (Fig. 3A). The supernatant from the *amiC* and *nlpD* complementation strains showed partial phenotypic complementation, with 2- and 3-times-higher NOD1 responses than those in the supernatant from the mutant strains, respectively ($P < 0.05$) (Fig. 3A).

We also treated a HEK293 cell line overexpressing human NOD2 in parallel with the same supernatant samples as the ones used for the NOD1 experiments (Fig. 3B). The

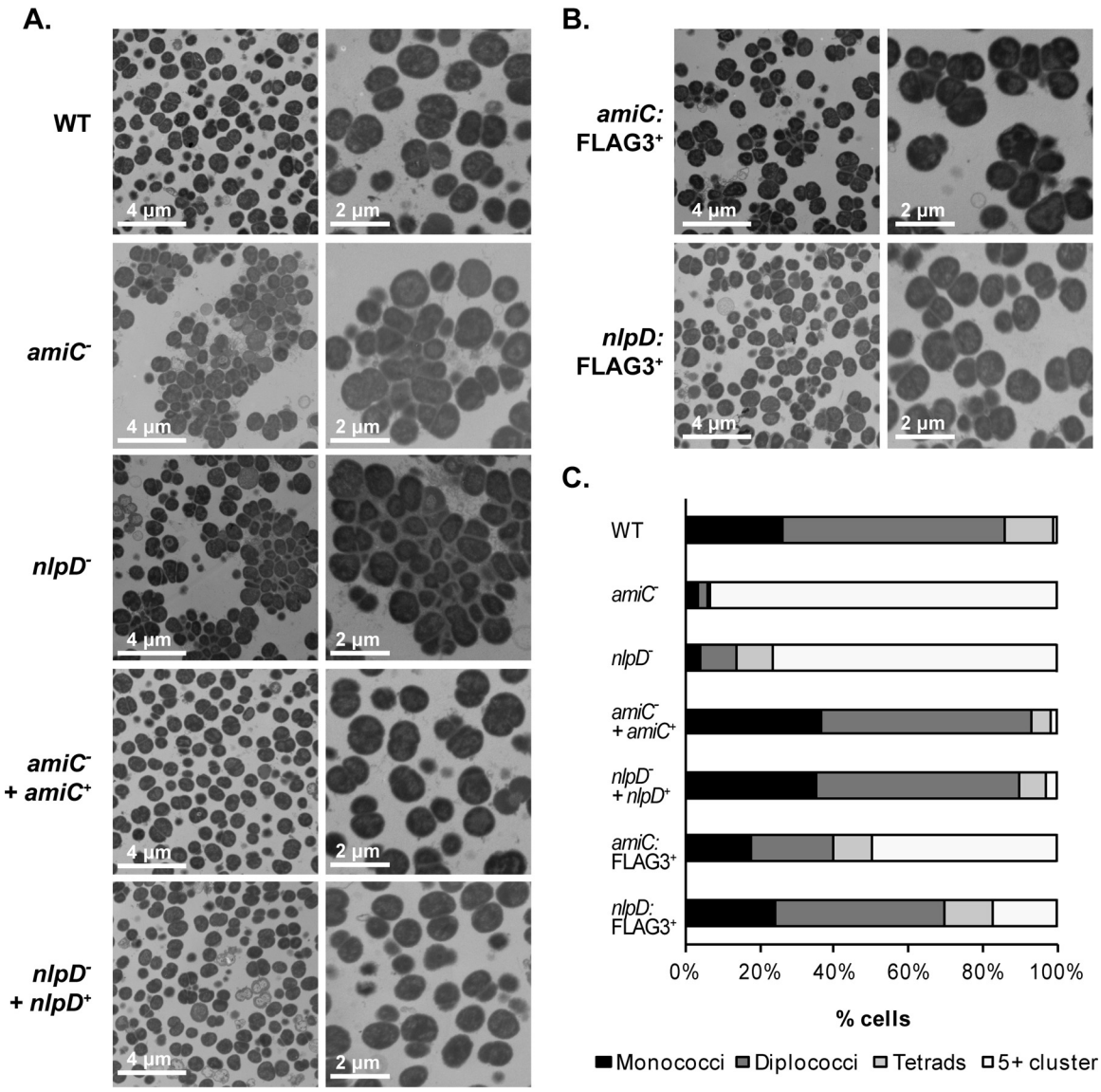

FIG 4 Cell separation defects in *amiC* or *nlpD* mutants. (A and B) WT, *amiC* mutant and complementation strains (KL1065 and EC1020), and *nlpD* mutant and complementation strains (KL1072 and EC1026) (A) as well as strains expressing *amiC*::*FLAG3*$^+$ (EC1032) and *nlpD*::*FLAG3*$^+$ (EC1033) (B) were imaged by thin-section transmission electron microscopy. (C) Quantification of the number of cells presenting as monococci, diplococci, tetrads, and clumps of 5 or more cells in 16 to 24 fields of view containing an average of 30 cells each was performed and is presented as a percentage of total cells.

intracellular innate immune receptor NOD2 recognizes muramyl dipeptide (MDP) and responds to reducing-end PG monomers, and thus, it would not be expected to be differentially affected by the amounts of free peptides (41–43). As predicted, treatment with the supernatant from *amiC* or *nlpD* mutants did not alter NOD2 activation levels. Thus, we conclude that PG-derived peptides generated by the action of AmiC and NlpD in *N. meningitidis* induce a NOD1 response but do not activate NOD2 in a human epithelial cell line.

AmiC and NlpD are required for cell separation. Periplasmic *N*-acetylmuramyl-L-alanine amidases that act on the sacculi cleave septal PG to allow proper cell separation (30, 44). To examine the role of meningococcal AmiC and NlpD in cell separation, we performed thin-section transmission electron microscopy (TEM) to visualize the cell morphology of the WT, mutant, and complementation strains. We counted the numbers of cells presenting as monococci, diplococci, tetrads, and clusters of 5 or more cells in 16 to 24 fields/strain. Each field used for quantification had an average of 30 cells; an example of a field for each strain used for quantification is shown in Fig. 4A. A

higher-magnification image demonstrating the size of the multicell clumps of the *amiC* and *nlpD* mutants is also included.

WT cells predominantly presented as diplococci (60%) and monococci (26%), with a few cells being found as tetrads (13%) and clusters of 5 or more cells (1%) (Fig. 4A and C). In contrast, both the *amiC* and *nlpD* mutants formed large aggregates of 5 cells or more (94% and 76%, respectively). Mutation of *amiC* caused a more severe cell separation defect than did mutation of *nlpD*, as more cells were found in large clusters and fewer cells were found as diplococci or monococci (Fig. 4A and C). Only 3% each of *amiC* mutant cells presented as diplococci and monococci, while 10% and 4% of *nlpD* mutants presented as diplococci and monococci, respectively (Fig. 4C). Both the *amiC* and *nlpD* complementation strains showed WT-like cell morphology, with most cells presenting as diplococci (57% and 55%, respectively) and monococci (37% and 35%, respectively) (Fig. 4C). We conclude that AmiC and NlpD are required for proper cell separation in *N. meningitidis*.

C-terminally FLAG3-tagged AmiC displays both septal and distributed localizations, while tagged NlpD is septally localized. We generated C-terminally triple-FLAG-epitope (FLAG3)-tagged versions of AmiC and NlpD to visualize the localization of these proteins in the cell via stochastic optical reconstruction microscopy (STORM). To determine the functionality of these tagged proteins, we performed TEM to look at the cell morphology of the *amiC*::*FLAG3*$^+$- and *nlpD*::*FLAG3*$^+$-expressing strains (Fig. 4B). The *nlpD*::*FLAG3*$^+$ strain predominantly presented as diplococci (46%) and monococci (24%), although it had more clusters of 5 or more cells than the WT (17% versus 1%). In contrast, *amiC*::*FLAG3*$^+$ cells were more likely to be found in clumps of 5 or more cells (50%), with only 22% and 18% of cells presenting as diplococci and monococci (Fig. 4C). However, the cell clumps in an *amiC*::*FLAG3*$^+$ mutant were much smaller and contained fewer cells than the large cell clusters formed by an *amiC* or an *nlpD* mutant, suggesting that AmiC::FLAG3 is partially functional for cell separation.

Localizations of AmiC::FLAG3 and NlpD::FLAG3 in *N. meningitidis* were determined using STORM, and chromosomal DNA was counterstained with 4′,6-diamidino-2-phenylindole (DAPI) and visualized by epifluorescence microscopy to determine the position of the cells. The presence of a signal band between two adjacent DAPI foci (cells) was interpreted as septal localization. We observed two types of localization patterns for AmiC::FLAG3 (Fig. 5). First, AmiC::FLAG3 localized to the putative septum in a small subset of cells (Fig. 5, left). Second, we observed a peripheral distribution of AmiC::FLAG3 for most cells in both diplococcal and larger aggregates. NlpD::FLAG3 was clearly localized to the septum in nearly all cells, with a few cells showing some staining that might extend beyond the septum (Fig. 5, right). Since the FLAG3 tag had some effects on the function of the two proteins (Fig. 4C), more so for AmiC and less so for NlpD, we cannot rule out an effect of the tag on protein localization. However, our observations are similar to the known recruitment of the *E. coli* AmiC and NlpD homologues to the septum during late cell division (39, 45). Peripheral distributions of AmiC and NlpD homologues in *E. coli* are also seen in nondividing cells, with a minor enrichment of *E. coli* AmiC at the poles of such cells (39). Our findings suggest that AmiC::FLAG3 localizes to the septum in dividing meningococcal cells and may be distributed around the cell in nondividing cells.

Infection of human whole blood. The severe cell separation defects of the *amiC* and *nlpD* mutants might be expected to affect infection, and differences in the release of PG fragments might affect phagocyte function. However, a significant difficulty in testing the infection ability of such mutants is the inability to accurately quantify the number of viable bacterial cells following infection since each CFU for the mutants contains multiple bacterial cells stuck together. To circumvent this difficulty, we used the *nlpD* mutant carrying an inducible complement construct. In the absence of the anhydrotetracycline inducer, the mutant grows as unseparated cell clusters. However, after 4 h of growth in medium containing anhydrotetracycline, a wild-type level of cell separation is achieved (Fig. 6A). Thus, we could get a reflection of CFU numbers from

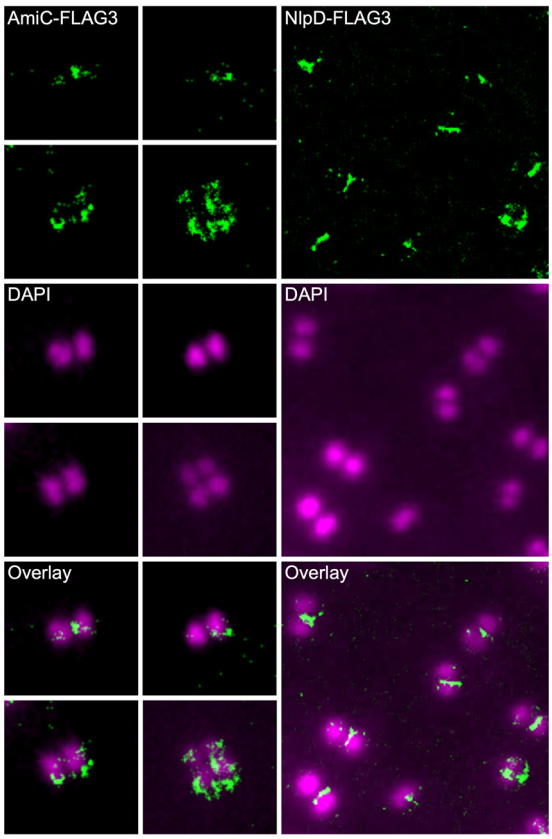

FIG 5 Localization of AmiC::FLAG3 and NlpD::FLAG3 in the meningococcal cell. Localizations of AmiC::FLAG3 or NlpD::FLAG3 were determined using STORM. DNA was counterstained with DAPI. The localization of AmiC::FLAG3 is presented in the left panels, and the localization of NlpD::FLAG3 is presented in the right panels. Septal localization of the proteins is seen when they form an approximate line between the two DAPI-stained cells of a diplococcus. As NlpD::FLAG3 exhibited nearly full functionality, a single field with multiple diplococci was easily found and is shown, whereas AmiC::FLAG3 was only partially functional, making it necessary to gather images of diplococci or small clumps from several fields.

infection by growing the bacteria from each time point with an inducer and then dilution plating the then-separated bacteria.

We compared the abilities of the WT strain and the *nlpD* mutant to survive in whole human blood. When we attempted this experiment in an encapsulated strain background, no difference was seen between the WT and the mutant. However, in unencapsulated strains, the *nlpD* mutant exhibited a substantial defect. Upon the addition of the bacteria to the blood, CFU numbers for the WT strain dropped, reaching ~50% by 2 h and then growing to 170% by 4 h (Fig. 6B). In contrast, the CFU of the *nlpD* mutant dropped 45-fold upon addition to blood and continued to decrease. By 4 h, the *nlpD* mutant CFU had dropped more than 2,000-fold. When we used cobra venom factor (CVF) to deplete complement in the blood before bacterial addition, the initial decrease in CFU numbers for the WT strain was eliminated, and the initial decrease for the *nlpD* mutant was reduced to only a 2-fold effect. After that point, the WT strain in the CVF-treated blood maintained CFU numbers for the first 2 h and then grew to >9-fold the starting value (Fig. 6B). The *nlpD* mutant in the CVF-treated blood died at the same rate as the *nlpD* mutant did in untreated blood albeit with CFU values 20- to 40-fold higher at each time point. A control experiment in which the WT or the *nlpD* mutant was incubated in diluted tissue culture medium demonstrated that the *nlpD* mutant is not defective in survival in nutrient-poor medium (see Fig. S1 in the supplemental material). When we incubated the WT or the *nlpD* mutant with human serum, the survival of the mutant was not significantly different from that of the WT and trended toward better survival for

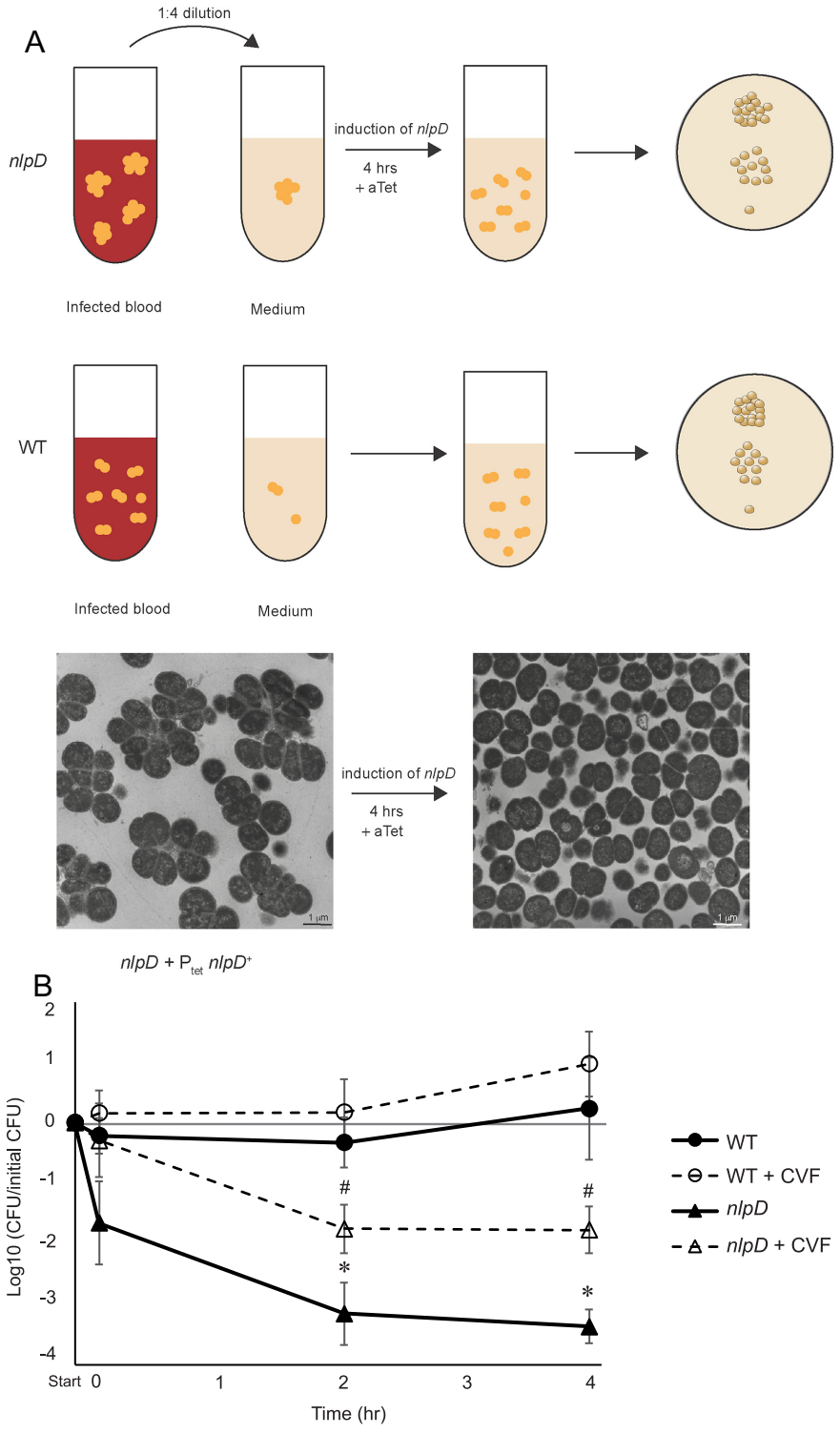

FIG 6 Survival in human whole blood. An *nlpD* mutant with a tightly regulated complementation construct (EC1026) was used to examine the effect of a cell separation defect on infection. (A) Schematic showing the method used for enumerating bacteria following blood infection. Approximately equal numbers of WT and mutant bacteria were used to infect human blood *in vitro*, although they give different CFU counts due to the *nlpD* mutant not separating. At each time point, the bacteria were diluted into GCBL medium containing anhydrotetracycline (aTet) to induce *nlpD* expression in the complemented strain, and after 4 h of growth, the bacteria were diluted and plated to determine CFU numbers. Thin-section transmission electron microscopy shows that EC1026 exhibits the cell separation defect without induction, but 4 h in the presence of anhydrotetracycline results in separation into individual diplococci and monococci. (B) The WT (ATCC 13102 *cap*) and *nlpD* mutant (EC1026) were

(Continued on next page)

the mutant (Fig. S2). Overall, these results demonstrate that the *nlpD* mutant has a defect in survival in human blood and that a large part of that defect is mediated by complement but not complement alone. Even when complement is depleted, the *nlpD* mutant also shows a survival defect, suggesting increased killing by other soluble factors or phagocytes.

DISCUSSION

These studies demonstrated that the major PG fragments released by *N. meningitidis* are PG-derived peptides, with the most abundant species being the free tripeptide and tetrapeptide. The tri- and tetrapeptides are also released in large amounts by the related species *N. gonorrhoeae*, although *N. meningitidis* releases much larger amounts of the peptides than *N. gonorrhoeae*. The peptides are generated by the action of the periplasmic *N*-acetylmuramyl-L-alanine amidase AmiC, which is activated by the outer membrane lipoprotein NlpD. Mutation of either *amiC* or *nlpD* in *N. meningitidis* completely abolished PG-derived peptide release (Fig. 2). AmiC and NlpD were also necessary for generating the free dipeptide. The enzyme responsible for dipeptide production has not been characterized in *Neisseria* spp., but three NlpC family endopeptidases are encoded in the meningococcal genome, and these enzymes generally function to cleave the γ-D-Glu-DAP bond (46). The requirement for AmiC and NlpD for making the dipeptide suggests that the tetrapeptide must first be cleaved from the glycan strand by AmiC before the endopeptidase can act on it. In support of this idea, some NlpC family enzymes have been found to require a free N-terminal L-alanine for peptides to serve as the substrates for these enzymes (34).

Mutation of *amiC* or *nlpD* led to a significant reduction in NOD1 activation. This result is consistent with the loss of free tripeptide release in these mutants. It is well established that human NOD1 responds to PG fragments containing γ-D-Glu-DAP and terminating with DAP, which would include the free tripeptide released by meningococci (18–20, 22). In studies of *N. gonorrhoeae*, abolishing neither free peptide release nor disaccharide-tripeptide monomer release reduced NOD1 activation, indicating that the production of either the tripeptides or the disaccharide-tripeptide monomers was sufficient for stimulating NOD1 (28). Our results with *N. meningitidis* indicate that the free tripeptides are the major NOD1 agonists for this species and emphasize that meningococci rely on the AmiC-mediated pathway for most PG degradation (Fig. 1 and 2). Meningococci release lower levels of tripeptide PG monomer than gonococci, and the meningococcal supernatant induces lower NOD1 activation in HEK293 cells and interleukin-8 (IL-8) production by Fallopian tube explants than the gonococcal supernatant (8). The increased release of PG monomers by gonococci is partly due to a somewhat defective version of AmpG, the PG fragment permease, leading to a decreased recycling efficiency for anhydro-disaccharide-containing PG fragments. However, *ampG* is not fully responsible for the differences in fragment release between gonococci and meningococci since the replacement of meningococcal *ampG* with that of gonococci only somewhat increased PG monomer release, and this meningococcal strain continued to show the more extensive degradation of PG fragments to free disaccharides and anhydro-muramic acid (36). Taken together with these previously reported observations, our results provide support to the hypothesis that *N. meningitidis* degrades PG fragments more extensively than *N. gonorrhoeae* and thereby reduces NOD1 activation, which may reduce immune clearance during asymptomatic colonization.

It is not currently clear how PG fragment release contributes to the meningococcal lifestyle. In response to a NOD1 agonist or other inflammatory molecules, oral epithelial

FIG 6 Legend (Continued)
inoculated into hirudin-treated human blood. Where indicated, CVF was used to deplete complement in the blood before inoculation. Because of the difficulties inherent in obtaining equal numbers of separating and not-separating bacteria for the initial inoculation, the data are plotted as the ratio of final CFU to initial CFU at each time point, on a log scale. Statistical significance was determined by Student's *t* test, in which * indicates a *P* value of <0.05 compared to the WT and # indicates a *P* value of <0.05 compared to the WT plus CVF. These data are the geometric means ± standard errors of the means from five independent experiments.

cells alter gene expression without inducing an inflammatory response (47). Still, it is not particularly surprising that PG fragments released by meningococci do not induce inflammation in nasopharyngeal tissue since asymptomatic colonization is by definition not overtly damaging to the host on the organismal level. Released PG fragments may play a role in establishing colonization, invading the meninges, exacerbating damage during invasive meningococcal disease, or colonizing new niches such as the urethra (11, 48).

Consistent with the role of AmiC as a cell separation amidase, mutation of *amiC* or *nlpD* led to cell separation defects, which manifested as large cell clusters containing more than 10 cells (Fig. 4). STORM analyses revealed that in a small subset of cells, AmiC::FLAG3 formed a banding pattern at the septum, suggesting a septal localization of this protein. In a larger subset of cells, AmiC::FLAG3 was found randomly distributed around the cell. The NlpD::FLAG3 signal was found to localize to the septum. Such localization patterns suggest that NlpD is a septal protein and that AmiC is recruited to the septum during cell division, as observed in other species of bacteria (39, 45, 49).

The growth of the *amiC* mutant and the *nlpD* mutant as large aggregates of cells led us to test whether the cell separation deficiency might alter infection proficiency. In other systems, bacterial variants that grow as filaments have been found to have a survival advantage over normal bacilli and to avoid phagocytic killing (50). However, gonococci defective for *amiC*, while not showing a growth defect, were sensitive to killing by deoxycholate, suggesting membrane instability (30). Also, a meningococcal mutant lacking *gna33* (*ltgC*) showed a cell separation defect and was unable to infect infant rats in a model of septicemia (32). We used a human whole-blood infection model and infected the blood with the WT strain or an *nlpD* mutant carrying an inducible *nlpD* expression construct. While the WT strain was able to survive and grow in blood, the *nlpD* mutant showed a >1,000-fold defect in survival over 4 h. The survival defect was still present, although substantially lessened, when blood depleted for complement was used for infections. Neither incubation in dilute medium nor incubation with human serum recapitulated the decreased survival phenotype. These results indicate that in addition to complement, other factors present in blood, such as phagocytes, are necessary for the increased death of the nonseparating mutant.

Overall, these studies demonstrated that *N. meningitidis* AmiC and NlpD are necessary for producing the free peptides released by the bacteria and that meningococci favor this pathway for cell wall degradation. AmiC and NlpD are necessary for cell separation, and a cell separation mutant is defective in survival in an *ex vivo* model of human blood infection.

MATERIALS AND METHODS

Bacterial strains and growth conditions. All strains used in this study are listed in Table 1. Except where indicated, all meningococcal strains used in the experiments are unencapsulated derivatives of *N. meningitidis* (ATCC 13102 *cap*), in which the capsule biosynthesis gene *siaD* has been interrupted with a chloramphenicol marker (8). These strains also have a point mutation in *rpsL* conferring streptomycin resistance (8). *N. meningitidis* strains were grown on gonococcal base medium (GCB) agar (Difco) plates at 37°C with 5% CO_2 or in gonococcal base liquid medium (Difco) with 0.042% bicarbonate (51) and Kellogg's supplements (52) (cGCBL) at 37°C with aeration. *Escherichia coli* strains were grown on LB agar (Difco) plates at 37°C or in LB liquid medium at 37°C. When needed, 10 μg/mL chloramphenicol, 10 μg/mL erythromycin, or 80 μg/mL kanamycin was added to *N. meningitidis* cultures. For *E. coli*, 100 μg/mL ampicillin, 25 μg/mL chloramphenicol, 500 μg/mL erythromycin, or 40 μg/mL kanamycin was added to the media when appropriate. When necessary, 0.1 mM or 1 mM isopropyl-β-D-thiogalactopyranoside (IPTG) or 2 ng/mL anhydrotetracycline was added to the media to induce the expression of a target gene.

Strain construction. *N. meningitidis* mutants were generated by spot transformation (53). Briefly, 20 μg of linearized plasmid DNA or the PCR product was spotted onto a GCB agar plate and allowed to dry. Subsequently, 5 to 10 piliated colonies were streaked over the DNA spots, and the plate was incubated overnight at 37°C with 5% CO_2. Successful transformants were either selected using antibiotics or identified by PCR screening. All transformants were confirmed by PCR and DNA sequencing. Due to the difficulty in transforming *amiC* and *nlpD* mutants, complementation strains were constructed by first transforming the WT with the complementation construct, followed by transforming the resulting strains with the deletion construct. EC1026 is the only strain generated by transformation with a PCR product. This PCR product was generated by PCR amplification of *nlpD* from WT *N. meningitidis* chromosomal DNA using primers NlpD DUS F and NlpD DUS R (Table 2), which resulted in a DNA fragment

TABLE 1 Strains and plasmids used in this study

Strain or plasmid	Description	Reference
N. meningitidis strains		
ATCC 13102 Str	ATCC 13102 *rpsL*K43R	56
ATCC 13102 *cap*	ATCC 13102 *rpsL*K43R *siaD*::*cat* (WT *N. meningitidis*)	8
KL1060	ATCC 13102 Str transformed with pKL25; ATCC 13102 Str Δ*amiC*::*ermC rpsL*	This study
KL1061	KL1060 transformed with pDG005; ATCC 13102 Str Δ*amiC*	This study
KL1065	KL1061 transformed with pHC10; ATCC 13102 *cap* Δ*amiC*	This study
KL1071	ATCC 13102 Str transformed with pKL38; ATCC 13102 Str Δ*nlpD*::*kan*	This study
KL1072	KL1071 transformed with pHC10; ATCC 13102 *cap* Δ*nlpD*::*kan*	This study
EC1018	ATCC 13102 *cap* transformed with pKL50; ATCC 13102 *cap* P_{IPTG}-*amiC*	This study
EC1020	EC1018 transformed with pEC140; ATCC 13102 *cap amiC*::*kan* P_{IPTG}-*amiC*	This study
EC1022	ATCC 13102 *cap* transformed with pKL49; ATCC 13102 *cap* P_{tet}-*nlpD*-rpsL*	This study
EC1024	EC1022 transformed with pKL38; ATCC 13102 *cap nlpD*::*kan* P_{tet}-*nlpD*-rpsL*	This study
EC1026	EC1024 transformed with PCR-amplified *nlpD*; ATCC 13102 *cap* Δ*nlpD*::*kan* P_{tet}-*nlpD*	This study
EC1032	ATCC 13102 *cap* transformed with pEC169; ATCC 13102 *cap amiC*::*FLAG3*$^+$	This study
EC1033	ATCC 13102 *cap* transformed with pEC173; ATCC 13102 *cap nlpD*::*FLAG3*$^+$-*kan*	This study
Plasmids		
pDG005	Markerless *amiC* deletion in pIDN3	30
pHC10	Serogroup C *siaD*::*cat*	57
pHSS6	Cloning vector; source of *aph3* gene (referred to as Kan^r)	58
pKC1	Positive/negative selection plasmid for *Neisseria* spp.; source of *rpsL*	59
pKH6	Cloning vector derived from pIDN1 and pGCC6	56
pKH99	Cloning vector derived from pHSS6 and pIDN2; source of Kan^r gene	56
pMR33	Complementation vector; IPTG inducible	60
pMR68	Complementation vector; anhydrotetracycline inducible	60
pMR100	Cloning vector pIDN3 with a C-terminal FLAG3 sequence	61
pKL24	*amiC* deletion insert from pDG005 into pKH6	This study
pKL25	*ermC rpsL* in pKL24; Δ*amiC*::*ermC rpsL* in pKH6	This study
pKL28	*nlpD* and flanking DNA in pKH6	This study
pKL29	Markerless *nlpD* deletion in pIDN3; Δ*nlpD* in pIDN3	This study
pKL38	Kan^r in pKL29; Δ*nlpD*::*kan* in pIDN3	This study
pKL45	*nlpD** in pMR68 (has a premature stop codon)	This study
pKL49	*nlpD*-rpsL* in pMR68	This study
pKL50	*amiC* in pMR33	This study
pEC140	Kan^r from pHSS6 in pDG005; Δ*amiC*::*kan* in pIDN3	This study
pEC167	*amiC* 3′ flank in pMR100	This study
pEC168	*nlpD* 3′ flank in pMR100	This study
pEC169	Partial *amiC* coding sequence (*amiC*′) in pEC167; *amiC*′::*FLAG3*$^+$-3′ flank in pIDN3	This study
pEC170	Partial *nlpD* coding sequence (*nlpD*′) in pEC168	This study
pEC173	Kan^r in pEC170; *nlpD*′::*FLAG3*$^+$-Kan^r-3′ flank in pIDN3	This study

containing the *nlpD* coding sequence flanked by DNA uptake sequences (DUSs) to facilitate uptake and recombination (54). Transformation with this PCR product corrected the *nlpD* sequence at the complementation locus to the WT sequence.

Plasmid construction. All plasmids used in this study are listed in Table 1 and were verified by PCR and sequencing. All primers are listed in Table 2. Plasmids were generated by the ligation of a vector backbone and an insert and transformed into Rapid Trans chemically competent TAM1 cells (Active Motif).

Two plasmids, pKL24 and pKL25, were generated to create an in-frame deletion of *amiC*. To make pKL24 (*amiC* deletion in pKH6), pDG005 and pKH6 were digested with XmaI and SacI. The *amiC* deletion insert from pDG005 was ligated into pKH6, generating pKL24. To generate pKL25 (*ermC rpsL* in pKL24; final construct, Δ*amiC*::*ermC rpsL*), the *ermC rpsL* positive/negative selection cassette was first excised from pKC1 by digestion with NheI and EcoRV. The insert from pKC1 was blunted with T4 polymerase and ligated into the blunted BspHI site from pKL24 to create pKL25.

Three plasmids were generated to create an *nlpD* insertional inactivation mutant. To create pKL28 (*nlpD* and flanking DNA in pKH6), PCR was used to amplify *nlpD* and flanking DNA with primers SacII nlpD F and SacI nlpD R. The PCR product and pKH6 were digested with SacI and SacII and then ligated. To generate pKL29 (*nlpD* deletion in pKH6), primers BglII nlpD del F and BglII nlpD del R were used for PCR with pKL28 as a template. The product was digested with BglII and self-ligated to make pKL29, which contains a markerless *nlpD* deletion with flanking DNA. To build pKL38 (Δ*nlpD*::*kan* allelic replacement in pKH6), the kanamycin resistance (Kan^r) marker from pKH99 was excised by digestion with EcoRV and Ecl136II and inserted into the blunted BglII site of pKL29.

Two plasmids, pKL45 and pKL49, were constructed to complement an *nlpD* mutation at an ectopic site. Plasmid pKL45 (*nlpD** in pMR68) was made by first amplifying *nlpD* from WT *N. meningitidis* chromosomal

TABLE 2 Primers used in this study

Primer	Sequence[a]
SacII nlpD F	TAACCGCGGAGGCACTGTGGACATTGTTG
SacI nlpD R	GATTGAGCTCTCACGATGGTTGCGGTCAAAG
BglII nlpD del F	GCCGAGATCTAGCTATATCGCGTTCTGACTTTC
BglII nlpD del R	GCCCAGATCTCATAAGATAACCTTCATGTTCCG
SacI nlpD F2	GCCGGAGCTCATCGGAACATGAAGGTTATC
SpeI nlpD R	GCCGACTAGTGATTTCAGGCAGAAAGTCAG
MluI rpsL F	AATAACGCGTCCGCTCTTGCCGACATGGTG
MluI rpsL R	AATACGCGTTAGGCGGCCGACGTGCCTAATTG
SacI MC amiC F	TAATGAGCTCCCGAACGAGGACGCGAAAGCC
SpeI MC amiC R	GCCGACTAGTACCGCCTTTTCAATCAACCC
Kan F BamHI	CAGGATCCAAAGCCAGTCCGCAGAAACG
Kan R BamHI	CTGGATCCTGGGCGAAGAACTCCAGCAT
NlpD DUS F	ATGCCGTCTGAACTTTGCGCTTGAGAAGAACG
NlpD DUS R	TCTGTACTGTCTGCGGCTTC
SacI MC amiC-sigseq F	GATTAGAGCTCAAAACGGTACGCGCACCAC
EcoRI MC amiC-stop codon R	GTGCAGAATTCACCCCGCTTCAATACGGATG
HindIII amiC down F	GCACGAAGCTTTAGTTGTCGGATGAAGGCAG
XhoI amiC down R	GACGACTCGAGCAACCATTTCAATTCCGTATCC
SacI MC nlpD-sigseq F	GATTAGAGCTCGCTACCCAGCAGCCTGCC
EcoRI MC nlpD-stop codon R	GCGCAGAATTCGAACGCGATATAGCTGTTC
HindIII nlpD down F	GCAGCAAGCTTCTGCCTGAAATCAAGTTGG
XhoI nlpD down R	GATTACTCGAGATCGGCATCCGTGTCGAAGC

[a]Restriction enzyme sites are underlined.

DNA with primers SacI nlpD F2 and SpeI nlpD R. The PCR product and pMR68 were subsequently digested with SacI and SpeI and ligated to each other. Despite repeated attempts, the resulting plasmid contained one or more mutations in the *nlpD* coding sequence. We deduce that the presence of a second copy of *nlpD* in *E. coli* is toxic to the bacterium and saved one of the plasmids as pKL45. pKL45 has a nonsense mutation leading to a premature stop codon at the third codon. Plasmid pKL49 (*nlpD*-rpsL* in pMR68) was generated by the insertion of *rpsL* into pKL48. *rpsL* was amplified from pKC1 using primers MluI rspL F and MluI rpsL R; the PCR product and pKL45 were digested with MluI and subsequently ligated to each other to generate pKL49.

Plasmid pKL50 was generated to complement an *amiC* mutation at an ectopic site. To make pKL50 (*amiC* in pMR33), *amiC* was amplified from WT *N. meningitidis* chromosomal DNA with primers SacI MC amiC F and SpeI MC amiC R and digested with SacI and SpeI. pMR33 was digested similarly and ligated with the digested *amiC* PCR product.

Plasmid pEC140 was built to create a deletion/insertion mutant where *kan* replaced *amiC*. To generate pEC140 (*amiC*::*kan* in pIDN3), pDG005 was first digested with BspHI and subsequently blunted with T4 DNA polymerase. The *aph3* gene conferring resistance against kanamycin (referred to as the Kan^r gene) was amplified from pHSS6 using primers kan F BamHI and kan R BamHI and blunt ligated with the blunted, BspHI-digested pDG005 to form pEC140.

To epitope tag *amiC* at the native locus, pEC169 (*amiC*′::*FLAG3*$^+$-3′ flank in pIDN3) was constructed in multiple steps. First, the *amiC* 3′-flanking region was amplified using primers HindIII MC amiC down F and XhoI MC amiC down R and WT *N. meningitidis* chromosomal DNA as a template. pMR100 and the PCR product were digested with HindIII and XhoI and ligated to make pEC167 (*amiC* 3′ flank in pMR100). The partial coding sequence of *amiC* lacking the start codon, signal sequence, and stop codon (*amiC*′) was amplified from WT *N. meningitidis* DNA using primers SacI MC amiC-sigseq F and EcoRI MC amiC-stop codon R, digested with SacI and EcoRI, and ligated into similarly digested pEC167 to form pEC169.

To epitope tag *nlpD* at the native locus, pEC173 (*nlpD*′::*FLAG3*$^+$-Kan^r-3′ flank in pIDN3) was generated with a strategy similar to that for pEC169. The *nlpD* 3′-flanking region was amplified using primers HindIII MC nlpD down F and XhoI MC nlpD down R instead, digested with HindIII and XhoI, and ligated with similarly digested pMR100 to form pEC168. The partial coding sequence of *nlpD* lacking the start codon, signal sequence, and stop codon (*nlpD*′) was amplified with primers SacI MC nlpD-sigseq F and EcoRI MC nlpD-stop codon R, digested with SacI and EcoRI, and ligated into similarly digested pEC168 to form pEC170. pEC170 was digested with HindIII, blunted with T4 polymerase, and ligated with the Kan^r gene to form pEC173.

Metabolic labeling of peptidoglycan and quantitative fragment release. Metabolic labeling of PG and quantitative fragment release were performed as described previously (55). Strains were pulse-chase labeled with 25 μg/mL [2,6-^{3}H]DAP in Dulbecco's modified Eagle's medium (DMEM) lacking cysteine and supplemented with 100 μg/mL methionine and 100 μg/mL threonine for 45 min. A sample of the culture was removed to determine the number of radioactive counts per minute (cpm) by liquid scintillation counting, and the bacteria were diluted to obtain equal cpm in each culture. After a 2-h chase period, the supernatant was harvested by centrifuging the culture at 3,000 $\times$ *g* for 10 min and

filter sterilizing the supernatant with a 0.22-μm filter. [2,6-^{3}H]DAP-labeled molecules in the filtered supernatant were then separated using tandem size exclusion chromatography with 0.1 M LiCl as the mobile phase and detected by liquid scintillation counting. The growth media for the *amiC* and *nlpD* complementation strains were supplemented with 0.1 mM IPTG and 2 ng/mL anhydrotetracycline, respectively.

Thin-section transmission electron microscopy. *N. meningitidis* strains were grown in cGCBL until mid-log phase, when cells were harvested by centrifugation at 17,000 $\times$ *g* for 1 min. Growth medium for the *amiC* or *nlpD* complementation strain contained 0.1 mM IPTG or 2 ng/mL anhydrotetracycline, respectively, for gene induction. Cells were washed once with phosphate-buffered saline (PBS) and resuspended in a fixative solution (2% paraformaldehyde and 2.5% glutaraldehyde in 0.1 M phosphate buffer). Thin-section electron microscopy of fixed samples was done at the University of Wisconsin—Madison Medical School Electron Microscope Facility. Enumeration of meningococci in cell clusters was done by counting the number of complete, in-plane cells presenting as monococci, diplococci, tetrads, or clusters of five or more cells in 16 to 24 fields/strain containing an average of 30 cells/field.

Treatment of the HEK293 reporter cell line with the filtered supernatants from meningococcal cultures. HEK293-Blue cells that encode secreted alkaline phosphatase (SEAP) under the control of an NF-κB promoter (parental cell lines NULL1 and NULL2) and hNOD1 or hNOD2 receptors (NOD and NOD2 cell lines) were grown, maintained, and treated according to the manufacturer's instructions (InvivoGen). Supernatant samples were harvested from meningococcal cultures started at an optical density at 540 nm (OD_{540}) of 0.2, grown for 2 h by centrifugation at 17,000 $\times$ *g* for 1 min, and filter sterilized using a 0.22-μm-pore-size filter. Cultures were supplemented with 1 mM IPTG or 2 ng/mL anhydrotetracycline as needed. Supernatant samples were normalized to total cellular protein. HEK293 cells that were seeded at a density of 2.8 $\times$ 10^5 cells/mL (NOD1/NULL1) or 1.4 $\times$ 10^5 cells/mL (NOD2/NULL2) in 180 μL of DMEM with 4.5 g/L glucose, 2 mM L-glutamine, and 10% heat-inactivated fetal bovine serum (FBS) were treated with 20 μL of the supernatant for 18 h at 37°C with 5% CO_2. A total volume of 20 μL each of cGCBL (medium-only control), 10 μg/mL TriDAP (positive control for NOD1/NULL1) (InvivoGen), 10 μg/mL muramyl dipeptide (MDP) (positive control for NOD2/NULL2) (InvivoGen), 10 μg/mL Tri-Lys (negative control for NOD1/NULL1), or 10 μg/mL MDP-control (MDP-c) (negative control for NOD2/NULL2) (InvivoGen) was used as a treatment control. After 18 h of treatment, 20 μL of the HEK293 culture supernatant was added to 180 μL of QUANTI-Blue reagent (InvivoGen) and incubated at 37°C for 4 h. SEAP activity was determined by measuring the absorbance at 650 nm. To calculate NF-κB-dependent hNOD activation (graphed SEAP levels [A_{650}]), A_{650} values from NULL1 or NULL2 controls were subtracted from the corresponding A_{650} values from NOD1 or NOD2 treatments. The results are from four independent experiments, and statistical tests were performed using Student's *t* test.

Stochastic optical reconstruction microscopy. Sample preparation and imaging were done as described previously (23). Meningococcal cultures were grown to mid-log phase and harvested by centrifugation at 17,000 $\times$ *g* for 2 min. Cells were washed once with PBS and suspended in 400 μL of a fixative solution (4% methanol-free formaldehyde in PBS). The cell suspensions were incubated first at room temperature (RT) for 15 min and then on ice for 15 min. The cell suspensions were then centrifuged at 6,000 $\times$ *g*, and the fixative solution was discarded. Cells were quickly washed three times with cold PBS to ensure the thorough removal of the fixative solution, resuspended in cold GTE buffer (50 mM glucose, 1 mM EDTA, 20 mM Tris-HCl [pH 7.5]), and incubated on ice for 10 min. Cells were quickly washed with PBS-T (0.3% Triton X-100 in PBS), suspended in cold methanol, and incubated at $-$20°C for a minimum of 10 min. Methanol was removed, after which cells were washed with PBS-T for 5 min, blocked with 400 μL 5% goat serum in PBS-T for 15 min, and incubated with 1:150-diluted M2 primary antibody (Sigma) in PBS for 1 h. Cells were subsequently washed with PBS three times and incubated with 200 μL 1:100-diluted Alexa Fluor 647 (Thermo Fisher) secondary antibody, 100 ng/mL DAPI, and 5% goat serum in PBS for 1 h at RT or overnight at 4°C. Cells were washed with PBS five times to remove unbound antibody and dye suspended in 200 μL PBS. Around 2-μL volumes of the samples were spotted onto poly-L-lysine-coated coverslips, mounted with Vectashield H-1000 mounting medium (Vector Laboratories), and visualized using a Nikon N-Storm microscope. Images were analyzed using NIS-Elements AR software with N-Storm analysis. Linear brightness/contrast adjustments and false coloring were performed using FIJI.

Human blood infection assay. Blood was collected from healthy donors using hirudin-containing vacutainer tubes (48). All human subjects gave written informed consent in accordance with a protocol approved by the University of Wisconsin—Madison Health Sciences Institutional Review Board (protocol number 2017-1179). *N. meningitidis* was grown overnight on a GCB agar plate and harvested into phosphate-buffered saline. The blood was inoculated with *N. meningitidis* strains at 1 $\times$ 10^8 CFU/mL bacteria, and the cultures were grown with rotation at 37°C. To enumerate *N. meningitidis* used as the inoculum at the start of the experiment, the bacteria were inoculated into cGCBL instead of blood and dilution plated. In contrast, time zero was the time point taken immediately after the inoculation of the blood. Where indicated, blood was pretreated with 1 μg/mL cobra venom factor for 1 h prior to inoculation, with the blood culture rotating at 37°C. At each time point, 375 μL of each blood culture was removed and diluted into 1.125 mL of cGCBL medium. Anhydrotetracycline (final concentration of 2 ng/mL) was added to each culture. The diluted cultures were grown at 37°C for 4 h to allow expression from the complementation construct. After 4 h, the bacteria were diluted and plated for CFU determinations. Incubations in dilute medium were performed in the same manner as for blood except that the bacteria were suspended in DMEM diluted 1:8 in phosphate-buffered saline.

Serum resistance assay. *N. meningitidis* cells were suspended in cGCBL and grown for 2 h with aeration to reach log phase. Log-phase bacteria were diluted to an OD_{540} of 0.2 in DMEM. Four 1:10 dilutions of the culture were performed, and the fourth dilution was treated with 25% human serum at 37°C. At 0

and 30 min, 25 μL of each culture was plated for CFU counts. To prepare the heat-killed control serum, the serum was incubated at 56°C for 30 min.

SUPPLEMENTAL MATERIAL

Supplemental material is available online only.

SUPPLEMENTAL FILE 1, PDF file, 0.2 MB.

ACKNOWLEDGMENTS

This work was supported by National Institute of Allergy and Infectious Diseases grant R01AI097157 to J.P.D.

We acknowledge Ben August from the UW-Madison Medical School EM Facility for assistance with TEM and Elle Kielar-Grevstad from the UW-Madison Biochemistry Optical Core for advice and technical assistance on STORM.

REFERENCES

1. Cohn AC, MacNeil JR, Harrison LH, Hatcher C, Theodore J, Schmidt M, Pondo T, Arnold KE, Baumbach J, Bennett N, Craig AS, Farley M, Gershman K, Petit S, Lynfield R, Reingold A, Schaffner W, Shutt KA, Zell ER, Mayer LW, Clark T, Stephens D, Messonnier NE. 2010. Changes in *Neisseria meningitidis* disease epidemiology in the United States, 1998-2007: implications for prevention of meningococcal disease. Clin Infect Dis 50:184–191. https://doi.org/10.1086/649209.
2. Kirsch EA, Barton RP, Kitchen L, Giroir BP. 1996. Pathophysiology, treatment and outcome of meningococcemia: a review and recent experience. Pediatr Infect Dis J 15:967–978. https://doi.org/10.1097/00006454-199611000-00009.
3. Stephens DS, Greenwood B, Brandtzaeg P. 2007. Epidemic meningitis, meningococcaemia, and *Neisseria meningitidis*. Lancet 369:2196–2210. https://doi.org/10.1016/S0140-6736(07)61016-2.
4. Yezli S, Wilder-Smith A, Bin Saeed AA. 2016. Carriage of *Neisseria meningitidis* in the Hajj and Umrah mass gatherings. Int J Infect Dis 47:65–70. https://doi.org/10.1016/j.ijid.2015.11.014.
5. Pizza M, Rappuoli R. 2015. *Neisseria meningitidis*: pathogenesis and immunity. Curr Opin Microbiol 23:68–72. https://doi.org/10.1016/j.mib.2014.11.006.
6. Johswich K. 2017. Innate immune recognition and inflammation in *Neisseria meningitidis* infection. Pathog Dis 75:ftx022. https://doi.org/10.1093/femspd/ftx022.
7. Doran KS, Fulde M, Gratz N, Kim BJ, Nau R, Prasadarao N, Schubert-Unkmeir A, Tuomanen EI, Valentin-Weigand P. 2016. Host-pathogen interactions in bacterial meningitis. Acta Neuropathol 131:185–209. https://doi.org/10.1007/s00401-015-1531-z.
8. Woodhams KL, Chan JM, Lenz JD, Hackett KT, Dillard JP. 2013. Peptidoglycan fragment release from *Neisseria meningitidis*. Infect Immun 81:3490–3498. https://doi.org/10.1128/IAI.00279-13.
9. Vollmer W, Blanot D, de Pedro MA. 2008. Peptidoglycan structure and architecture. FEMS Microbiol Rev 32:149–167. https://doi.org/10.1111/j.1574-6976.2007.00094.x.
10. Schleifer KH, Kandler O. 1972. Peptidoglycan types of bacterial cell walls and their taxonomic implications. Bacteriol Rev 36:407–477. https://doi.org/10.1128/br.36.4.407-477.1972.
11. Höltje JV. 1995. From growth to autolysis: the murein hydrolases in *Escherichia coli*. Arch Microbiol 164:243–254. https://doi.org/10.1007/BF02529958.
12. Rosenthal RS. 1979. Release of soluble peptidoglycan from growing gonococci: hexaminidase and amidase activities. Infect Immun 24:869–878. https://doi.org/10.1128/iai.24.3.869-878.1979.
13. Park JT, Uehara T. 2008. How bacteria consume their own exoskeletons (turnover and recycling of cell wall peptidoglycan). Microbiol Mol Biol Rev 72:211–227. https://doi.org/10.1128/MMBR.00027-07.
14. Johnson JW, Fisher JF, Mobashery S. 2013. Bacterial cell-wall recycling. Ann N Y Acad Sci 1277:54–75. https://doi.org/10.1111/j.1749-6632.2012.06813.x.
15. Chan JM, Dillard JP. 2017. Attention seeker: production, modification, and release of inflammatory peptidoglycan fragments in *Neisseria* species. J Bacteriol 199:e00354-17. https://doi.org/10.1128/JB.00354-17.
16. Heiss LN, Moser SA, Unanue ER, Goldman WE. 1993. Interleukin-1 is linked to the respiratory epithelial cytopathology of pertussis. Infect Immun 61:3123–3128. https://doi.org/10.1128/iai.61.8.3123-3128.1993.
17. Melly MA, McGee ZA, Rosenthal RS. 1984. Ability of monomeric peptidoglycan fragments from *Neisseria gonorrhoeae* to damage human fallopian-tube mucosa. J Infect Dis 149:378–386. https://doi.org/10.1093/infdis/149.3.378.
18. Chamaillard M, Hashimoto M, Horie Y, Masumoto J, Qiu S, Saab L, Ogura Y, Kawasaki A, Fukase K, Kusumoto S, Valvano MA, Foster SJ, Mak TW, Nunez G, Inohara N. 2003. An essential role for NOD1 in host recognition of bacterial peptidoglycan containing diaminopimelic acid. Nat Immunol 4:702–707. https://doi.org/10.1038/ni945.
19. Girardin SE, Boneca IG, Carneiro LA, Antignac A, Jehanno M, Viala J, Tedin K, Taha MK, Labigne A, Zahringer U, Coyle AJ, DiStefano PS, Bertin J, Sansonetti PJ, Philpott DJ. 2003. Nod1 detects a unique muropeptide from gram-negative bacterial peptidoglycan. Science 300:1584–1587. https://doi.org/10.1126/science.1084677.
20. Girardin SE, Travassos LH, Herve M, Blanot D, Boneca IG, Philpott DJ, Sansonetti PJ, Mengin-Lecreulx D. 2003. Peptidoglycan molecular requirements allowing detection by Nod1 and Nod2. J Biol Chem 278:41702–41708. https://doi.org/10.1074/jbc.M307198200.
21. Ghosh M, Shen Z, Fahey JV, Crist SG, Patel M, Smith JM, Wira CR. 2013. Pathogen recognition in the human female reproductive tract: expression of intracellular cytosolic sensors NOD1, NOD2, RIG-1, and MDA5 and response to HIV-1 and *Neisseria gonorrhea* [*sic*]. Am J Reprod Immunol 69:41–51. https://doi.org/10.1111/aji.12019.
22. Vijayrajratnam S, Pushkaran AC, Balakrishnan A, Vasudevan AK, Biswas R, Mohan CG. 2016. Bacterial peptidoglycan with amidated meso-diaminopimelic acid evades NOD1 recognition: an insight into NOD1 structure-recognition. Biochem J 473:4573–4592. https://doi.org/10.1042/BCJ20160817.
23. Schaub RE, Chan YA, Lee M, Hesek D, Mobashery S, Dillard JP. 2016. Lytic transglycosylases LtgA and LtgD perform distinct roles in remodeling, recycling and releasing peptidoglycan in *Neisseria gonorrhoeae*. Mol Microbiol 102:865–881. https://doi.org/10.1111/mmi.13496.
24. Chan YA, Hackett KT, Dillard JP. 2012. The lytic transglycosylases of *Neisseria gonorrhoeae*. Microb Drug Resist 18:271–279. https://doi.org/10.1089/mdr.2012.0001.
25. Schaub RE, Perez-Medina KM, Hackett KT, Garcia DL, Dillard JP. 2019. *Neisseria gonorrhoeae* PBP3 and PBP4 facilitate NOD1 agonist peptidoglycan fragment release and survival in stationary phase. Infect Immun 87:e00833-18. https://doi.org/10.1128/IAI.00833-18.
26. Woodhams KL. 2013. Characterization of the gonococcal genetic island and peptidoglycan fragment release in Neisseria meningitidis. PhD thesis. University of Wisconsin—Madison, Madison, WI.
27. Lenz JD, Hackett KT, Dillard JP. 2017. A single dual-function enzyme controls the production of inflammatory NOD agonist peptidoglycan fragments by *Neisseria gonorrhoeae*. mBio 8:e01464-17. https://doi.org/10.1128/mBio.01464-17.
28. Lenz JD, Stohl EA, Robertson RM, Hackett KT, Fisher K, Xiong K, Lee M, Hesek D, Mobashery S, Seifert HS, Davies C, Dillard JP. 2016. Amidase activity of AmiC controls cell separation and stem peptide release and is enhanced by NlpD in *Neisseria gonorrhoeae*. J Biol Chem 291:10916–10933. https://doi.org/10.1074/jbc.M116.715573.
29. Stohl EA, Lenz JD, Dillard JP, Seifert HS. 2016. The gonococcal NlpD protein facilitates cell separation by activating peptidoglycan cleavage by AmiC. J Bacteriol 198:615–622. https://doi.org/10.1128/JB.00540-15.

30. Garcia DL, Dillard JP. 2006. AmiC functions as an *N*-acetylmuramyl-L-alanine amidase necessary for cell separation and can promote autolysis in *Neisseria gonorrhoeae*. J Bacteriol 188:7211–7221. https://doi.org/10.1128/JB.00724-06.
31. Cloud KA, Dillard JP. 2004. Mutation of a single lytic transglycosylase causes aberrant septation and inhibits cell separation of *Neisseria gonorrhoeae*. J Bacteriol 186:7811–7814. https://doi.org/10.1128/JB.186.22.7811-7814.2004.
32. Adu-Bobie J, Lupetti P, Brunelli B, Granoff D, Norais N, Ferrari G, Grandi G, Rappuoli R, Pizza M. 2004. GNA33 of *Neisseria meningitidis* is a lipoprotein required for cell separation, membrane architecture, and virulence. Infect Immun 72:1914–1919. https://doi.org/10.1128/IAI.72.4.1914-1919.2004.
33. Bhoopalan SV, Piekarowicz A, Lenz JD, Dillard JP, Stein DC. 2016. *nagZ* triggers gonococcal biofilm disassembly. Sci Rep 6:22372. https://doi.org/10.1038/srep22372.
34. Xu Q, Mengin-Lecreulx D, Liu XW, Patin D, Farr CL, Grant JC, Chiu HJ, Jaroszewski L, Knuth MW, Godzik A, Lesley SA, Elsliger MA, Deacon AM, Wilson IA. 2015. Insights into substrate specificity of NlpC/P60 cell wall hydrolases containing bacterial SH3 domains. mBio 6:e02327-14. https://doi.org/10.1128/mBio.02327-14.
35. Sinha RK, Rosenthal RS. 1980. Release of soluble peptidoglycan from growing gonococci: demonstration of anhydro-muramyl-containing fragments. Infect Immun 29:914–925. https://doi.org/10.1128/iai.29.3.914-925.1980.
36. Chan JM, Dillard JP. 2016. *Neisseria gonorrhoeae* crippled its peptidoglycan fragment permease to facilitate toxic peptidoglycan monomer release. J Bacteriol 198:3029–3040. https://doi.org/10.1128/JB.00437-16.
37. Goodell EW, Schwarz U. 1985. Release of cell wall peptides into culture medium by exponentially growing *Escherichia coli*. J Bacteriol 162:391–397. https://doi.org/10.1128/jb.162.1.391-397.1985.
38. Dillard JP. 2014. Peptidoglycan metabolism and fragment production, p 96–113. *In* Davies JK, Kahler CM (ed), Pathogenic Neisseria: genomics, molecular biology and disease intervention. Caister Academic Press, Norfolk, United Kingdom.
39. Bernhardt TG, de Boer PAJ. 2003. The *Escherichia coli* amidase AmiC is a periplasmic septal ring component exported via the twin-arginine transport pathway. Mol Microbiol 48:1171–1182. https://doi.org/10.1046/j.1365-2958.2003.03511.x.
40. Uehara T, Parzych KR, Dinh T, Bernhardt TG. 2010. Daughter cell separation is controlled by cytokinetic ring-activated cell wall hydrolysis. EMBO J 29:1412–1422. https://doi.org/10.1038/emboj.2010.36.
41. Girardin SE, Boneca IG, Viala J, Chamaillard M, Labigne A, Thomas G, Philpott DJ, Sansonetti PJ. 2003. Nod2 is a general sensor of peptidoglycan through muramyl dipeptide (MDP) detection. J Biol Chem 278:8869–8872. https://doi.org/10.1074/jbc.C200651200.
42. Inohara N, Ogura Y, Fontalba A, Gutierrez O, Pons F, Crespo J, Fukase K, Inamura S, Kusumoto S, Hashimoto M, Foster SJ, Moran AP, Fernandez-Luna JL, Nunez G. 2003. Host recognition of bacterial muramyl dipeptide mediated through NOD2. Implications for Crohn's disease. J Biol Chem 278:5509–5512. https://doi.org/10.1074/jbc.C200673200.
43. Knilans KJ, Hackett KT, Anderson JE, Weng C, Dillard JP, Duncan JA. 2017. *Neisseria gonorrhoeae* lytic transglycosylases LtgA and LtgD reduce host innate immune signaling through TLR2 and NOD2. ACS Infect Dis 3:624–633. https://doi.org/10.1021/acsinfecdis.6b00088.
44. Heidrich C, Templin MF, Ursinus A, Merdanovic M, Berger J, Schwarz H, de Pedro MA, Höltje JV. 2001. Involvement of *N*-acetylmuramyl-L-alanine amidases in cell separation and antibiotic-induced autolysis of *Escherichia coli*. Mol Microbiol 41:167–178. https://doi.org/10.1046/j.1365-2958.2001.02499.x.
45. Tsang MJ, Yakhnina AA, Bernhardt TG. 2017. NlpD links cell wall remodeling and outer membrane invagination during cytokinesis in *Escherichia coli*. PLoS Genet 13:e1006888. https://doi.org/10.1371/journal.pgen.1006888.
46. Anantharaman V, Aravind L. 2003. Evolutionary history, structural features and biochemical diversity of the NlpC/P60 superfamily of enzymes. Genome Biol 4:R11. https://doi.org/10.1186/gb-2003-4-2-r11.
47. Uehara A, Sugawara Y, Kurata S, Fujimoto Y, Fukase K, Kusumoto S, Satta Y, Sasano T, Sugawara S, Takada H. 2005. Chemically synthesized pathogen-associated molecular patterns increase the expression of peptidoglycan recognition proteins via Toll-like receptors, NOD1 and NOD2 in human oral epithelial cells. Cell Microbiol 7:675–686. https://doi.org/10.1111/j.1462-5822.2004.00500.x.
48. Sprong T, Brandtzaeg P, Fung M, Pharo AM, Hoiby EA, Michaelsen TE, Aase A, van der Meer JW, van Deuren M, Mollnes TE. 2003. Inhibition of C5a-induced inflammation with preserved C5b-9-mediated bactericidal activity in a human whole blood model of meningococcal sepsis. Blood 102:3702–3710. https://doi.org/10.1182/blood-2003-03-0703.
49. Möll A, Dörr T, Alvarez L, Chao MC, Davis BM, Cava F, Waldor MK. 2014. Cell separation in *Vibrio cholerae* is mediated by a single amidase whose action is modulated by two nonredundant activators. J Bacteriol 196:3937–3948. https://doi.org/10.1128/JB.02094-14.
50. Horvath DJ, Jr, Li B, Casper T, Partida-Sanchez S, Hunstad DA, Hultgren SJ, Justice SS. 2011. Morphological plasticity promotes resistance to phagocyte killing of uropathogenic *Escherichia coli*. Microbes Infect 13:426–437. https://doi.org/10.1016/j.micinf.2010.12.004.
51. Morse SA, Bartenstein L. 1974. Factors affecting autolysis of *Neisseria gonorrhoeae*. Proc Soc Exp Biol Med 145:1418–1421. https://doi.org/10.3181/00379727-145-38025.
52. Kellogg DS, Jr, Peacock WL, Jr, Deacon WE, Brown L, Pirkle CL. 1963. *Neisseria gonorrhoeae*. I. Virulence genetically linked to clonal variation. J Bacteriol 85:1274–1279. https://doi.org/10.1128/jb.85.6.1274-1279.1963.
53. Dillard JP. 2011. Genetic manipulation of *Neisseria gonorrhoeae*. Curr Protoc Microbiol Chapter 4:Unit 4A.2. https://doi.org/10.1002/9780471729259.mc04a02s23.
54. Goodman SD, Scocca JJ. 1988. Identification and arrangement of the DNA sequence recognized in specific transformation of *Neisseria gonorrhoeae*. Proc Natl Acad Sci U S A 85:6982–6986. https://doi.org/10.1073/pnas.85.18.6982.
55. Garcia DL, Dillard JP. 2008. Mutations in *ampG* or *ampD* affect peptidoglycan fragment release from *Neisseria gonorrhoeae*. J Bacteriol 190:3799–3807. https://doi.org/10.1128/JB.01194-07.
56. Woodhams KL, Benet ZL, Blonsky SE, Hackett KT, Dillard JP. 2012. Prevalence and detailed mapping of the gonococcal genetic island in *Neisseria meningitidis*. J Bacteriol 194:2275–2285. https://doi.org/10.1128/JB.00094-12.
57. Ram S, Cox AD, Wright JC, Vogel U, Getzlaff S, Boden R, Li J, Plested JS, Meri S, Gulati S, Stein DC, Richards JC, Moxon ER, Rice PA. 2003. Neisserial lipooligosaccharide is a target for complement component C4b. Inner core phosphoethanolamine residues define C4b linkage specificity. J Biol Chem 278:50853–50862. https://doi.org/10.1074/jbc.M308364200.
58. Seifert HS, Chen EY, So M, Heffron F. 1986. Shuttle mutagenesis: a method of transposon mutagenesis for *Saccharomyces cerevisiae*. Proc Natl Acad Sci U S A 83:735–739. https://doi.org/10.1073/pnas.83.3.735.
59. Cloud KA, Dillard JP. 2002. A lytic transglycosylase of *Neisseria gonorrhoeae* is involved in peptidoglycan-derived cytotoxin production. Infect Immun 70:2752–2757. https://doi.org/10.1128/IAI.70.6.2752-2757.2002.
60. Ramsey ME, Hackett KT, Kotha C, Dillard JP. 2012. New complementation constructs for inducible and constitutive gene expression in *Neisseria gonorrhoeae* and *Neisseria meningitidis*. Appl Environ Microbiol 78:3068–3078. https://doi.org/10.1128/AEM.07871-11.
61. Ramsey ME, Hackett KT, Bender T, Kotha C, van der Does C, Dillard JP. 2014. TraK and TraB are conserved outer membrane proteins of the *Neisseria gonorrhoeae* type IV secretion system and are expressed at low levels in wild-type cells. J Bacteriol 196:2954–2968. https://doi.org/10.1128/JB.01825-14.